S−S Bond Mesolysis in α,α′-Dinaphthyl Disulfide Radical Anion Generated during γ-Radiolysis and Pulse Radiolysis in Organic Solution

Minoru Yamaji,*,† Sachiko Tojo,‡ Kazuyuki Takehira,† Seiji Tobita,† Mamoru Fujitsuka,‡ and Tetsuro Majima*,‡

Department of Chemistry, Gunma University, Kiryu 376-8515, Japan, and The Institute of Scientific and Industrial Research (SANKEN), Osaka University, Mihogaoka 8-1, Ibaraki, Osaka 567-0047, Japan

Received: July 19, 2006; In Final Form: October 17, 2006

A dissociation mechanism of the S−S bond in the α,α′-dinaphthyl disulfide radical anion ($NpSSNp^{\bullet-}$) in organic solution was investigated on the basis of transient absorption measurements and DFT calculations. $NpSSNp^{\bullet-}$ generated during γ-radiolysis of NpSSNp in MTHF at 77 K showed the absorption band at 430 nm, which shifted to 560 nm with an increase of the ambient temperature up to room temperature. With the aid of DFT calculations at the B3LYP/6-31G(d) level, the shift of the absorption band was interpreted in terms of molecular conformational changes of $NpSSNp^{\bullet-}$ due to the elongation of the S−S bond. It was observed that $NpSSNp^{\bullet-}$ dissociates into naphthylthiyl radical and thionaphtholate anion in organic solution with a first-order rate constant in the magnitude of 10^6 s^{-1}. From Arrhenius plots of the decay rate constants of $NpSSNp^{\bullet-}$ in a temperature range of 160−293 K, an activation energy for the S−S bond cleavage in $NpSSNp^{\bullet-}$ in solution was determined along with a frequency factor. Based on the state energies of $NpSSNp^{\bullet-}$ calculated at the B3LYP/6-31G(d) level, a Morse-like energy potential for the S−S bond cleavage of $NpSSNp^{\bullet-}$ is depicted as a function of the S−S bond distance.

1. Introduction

The sulfur−sulfur bond plays an important role in the tertiary structure of polypeptides or proteins.[1] Dialkyl or diaryl disulfides (RSSR, R = alkyl or aryl) behave as a radiation protection agent in biological systems as well as mercaptans (RSH) or thiyl radicals ($RS^{\bullet}$).[2,3] The stationary-state radiation chemistry,[4−7] EPR investigations[8−11] and a large number of pulse radiolysis studies of cystine and related compounds[12−16] have been carried out in aqueous solution. These studies have been focused on the formation and decay of the disulfide radical anion ($RSSR^{\bullet-}$) having a characteristic transient absorption with a maximum peak at 410 nm,[13a,15−19] and a molar absorption coefficient of 9400 dm^3 mol^{-1} cm^{-1} at 410 nm.[13b] This species is generally formed either by attachment of hydrated electrons, e_{aq}^-, generated from radiolysis in aqueous solutions

$$e_{aq}^- + RSSR \rightarrow RSSR^{\bullet-} \quad (1)$$

or from the oxidation of RSH and thiolate anion (RS^-), yielding $RS^{\bullet}$, which participates in the equilibrium of

$$RS^{\bullet} + RS^- \rightleftarrows RSSR^{\bullet-} \quad (2)$$

Cystine reacts with the hydrated electron with a rate constant of 1.3×10^{10} dm^3 mol^{-1} s^{-1} to form a radical anion.[20] This species decays with a first-order rate constant of 2.9×10^5 s^{-1} in the absence of RS^- and undergoes rupture of the disulfide linkage,[16a]

$$RSSR^{\bullet-} \rightarrow RS^{\bullet} + RS^- \quad (3)$$

Kinetic investigations on bimolecular electron transfer from an appropriate electron donor to RSSR in aqueous solution also showed that the radical anion as products of electron-transfer subsequently undergoes the S−S bond cleavage.[21−24] There are, however, the formation and decay mechanisms of the radical anions in organic solution where chemical properties of a large number of radical anions have not been investigated. Because aromatic disulfides are not very soluble in aqueous solution, the decay mechanism of their radical anions (eq 3) can be investigated only in organic solution. In the present work, α,α′-dinaphthyl disulfide (NpSSNp) is employed to understand details of the rupture of the S−S bond of NpSSNp radical anion ($NpSSNp^{\bullet-}$) during the pulse radiolysis of NpSSNp at various temperatures in DMF. The transient absorptions of the products (naphthylthiyl radical and naphthyl thiolate anion) from $NpSSNp^{\bullet-}$ expressed by eq 3 are compared with those obtained from the laser flash photolysis of NpSSNp.[25] On the basis of the DFT calculations for the state energies of $NpSSNp^{\bullet-}$, the dissociation potential surface is depicted as a function of the S−S bond distance.

2. Experimental Section

α,α′-Dinaphthyl disulfide (NpSSNp) was synthesized by oxidation of α-naphthalenethiol (Lancaster) in ethanol in the presence of KOH and aqueous H_2O_2. Crude NpSSNp was purified by passing it through a silica-gel column with a mixture of hexane/ethyl acetate (5:1) and repeatedly recrystallized from hexane. MTHF (Tokyo Kasei Kogyo) was distilled over CaH_2 before use. DMF (Kishida chemical spectra grade) was used as received. MTHF solutions of NpSSNp (5.0×10^{-3} M) were degassed by several freeze−pump−thaw cycles on a high-

* To whom correspondence should be addressed. E-mail: yamaji@chem.gunma-u.ac.jp (M.Y.), majima@sanken.osaka-u.ac.jp (T.M.).
† Gunma University.
‡ Osaka University.

10.1021/jp0645770 CCC: $33.50
Published on Web 11/23/2006

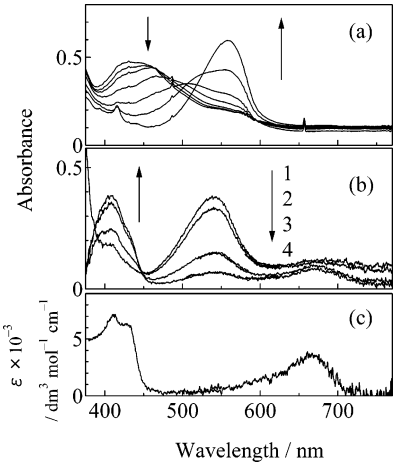

Figure 1. (a) Absorption spectra upon annealing from 77 to 100 K after γ-radiolysis of an MTHF rigid glass of NpSSNp for 30 min at 77K. (b) Transient absorption spectra observed at 50 ns (1), 100 ns (2), 500 ns (3) and 1 μs (4) after an electron pulse during the pulse radiolysis of NpSSNp in DMF at 293 K. (c) A reference absorption spectrum of NpS$^\bullet$ in acetonitrile.[23]

vacuum line (5×10^{-4} Torr) and sealed in a 1 cm path length Suprasil cell ($0.1 \times 1 \times 4$ cm^3). The concentration of NpSSNp was 5×10^{-3} mol dm^{-3} throughout this work.

γ-Radiolysis was carried out for 30 min with a ^{60}Co source at Osaka University. The dose rate was 4 kGy h^{-1}. Visible absorption spectra after γ-radiolysis of NpSSNp (5.0×10^{-3} M) in MTHF rigid glass were recorded on a spectrophotometer (Shimadzu Multispec-1500).

Transient absorption spectra of an argon-purged DMF solution of NpSSNp (5.0×10^{-3} M) in a Suprasil cell ($1 \times 1 \times 4$ cm^3) were obtained during the pulse radiolysis by using an electron pulse (28 MeV, 8 ns, 0.87 kGy pulse^{-1}) from a linear accelerator at Osaka University. The details of the detection system for transient absorption have been described elsewhere.[26] Transient absorption spectra were taken by using a photodiode array (Hamamatsu Photonics, S3904-1024F) with a gate image intensifier (Hamamatsu Photonics, C2925-01) as a detector. The temperature effects were determined using a cryostat (Oxford DN704) with a digital temperature controller (DTC-2) with precision of ± 1.0 °C.

The calculations were carried out at the density functional theory (DFT) level, using the Gaussian 03 software package.[27] The geometries of NpSSNp and NpSSNp$^{\bullet-}$ were fully optimized by using the 6-31G(d) base set at the B3LYP method.

3. Results and Discussion

Figure 1a shows absorption spectra upon annealing from 77 to 100 K obtained after the γ-radiolysis of an MTHF rigid glass of NpSSNp at 77 K. The absorption peak at 430 nm at 77 K is unambiguously assigned to be the NpSSNp radical anion (NpSSNp$^{\bullet-}$). Upon increasing the ambient temperature, the intensity of the absorption peak at 430 nm decreased, and a new peak at 570 nm appeared at 100 K. The absorption band at 540 nm was also seen in the transient absorption spectrum during the pulse radiolysis of NpSSNp in DMF at 295 K as shown in Figure 1b. The intensity of the absorption peak at 540 nm in DMF decreased with a decay rate constant (k_d) of 2.3×10^6 s^{-1} with an isosbestic point at 450 nm, and new absorption bands at 410 and 670 nm appeared with the same rate constant of 2.3×10^6 s^{-1} (Figure 2). A similar transient absorption spectrum was observed during the pulse radiolysis of NpSSNp in MTHF at 295 K.

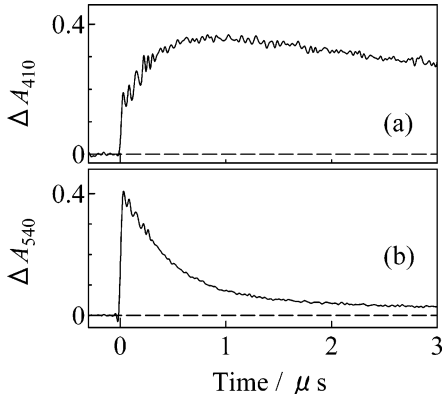

Figure 2. Time traces of the transient absorption at 410 nm (a) and 540 nm (b) obtained during the pulse radiolysis of NpSSNp in DMF at 293 K.

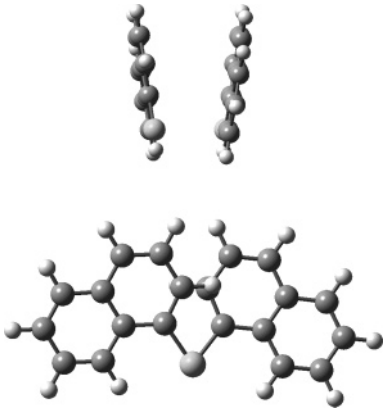

Figure 3. Views of the optimized conformation of NpSSNp$^{\bullet-}$ by using the B3LYP/6-31G(d) calculations. Upper: perpendicular to the S−S axial. Lower: parallel to the S−S axial.

The absorption spectrum observed 1 μs after an electron pulse was similar to that of the α-naphthylthiyl radical (NpS$^\bullet$),[28] as shown in Figure 1c. It is well-known that the S−S bond cleavage of RSSR$^{\bullet-}$ produces the corresponding thiyl radical and thiolate anion.[16a] Therefore, the absorption spectral changes in Figure 1b indicate that NpS$^\bullet$ is produced from the spontaneous S−S bond cleavage in NpSSNp$^{\bullet-}$, which has an absorption peak at 540 or 560 nm in THF or DMF, respectively, at room temperature. The absorption of the corresponding NpS$^\bullet$, that is, the α-thionaphtholate anion (NpS$^-$), was not seen in the wavelength region studied because NpS$^-$ absorbs at a shorter wavelength region than 380 nm. The obtained k_d value in DMF is comparable with or larger than those for cystine and related compounds in aqueous solution (10^5−10^6 s^{-1}).[16a]

By using DFT calculations, the shift of absorption bands upon annealing seen in Figure 1a was interpreted in terms of molecular conformational changes of NpSSNp$^{\bullet-}$ as a function of the S−S bond distance and the twist angle of the C−S−S−C bonding. The most significant geometrical parameters calculated for NpSSNp$^{\bullet-}$ and NpSSNp at the B3LYP/6-31G-(d) level show that the S−S bond of NpSSNp$^{\bullet-}$ is elongated to 0.290 nm compared with that of neutral NpSSNp (0.213 nm). The dihedral angle of the CSSC bonds for the optimized structure of NpSSNp$^{\bullet-}$ was 72.05° whereas that of NpSSNp was 78.38°. The optimized molecular geometry of NpSSNp$^{\bullet-}$ is depicted in Figure 3. The molecular conformation of NpSSNp$^{\bullet-}$ generated from radiolysis in a rigid matrix at 77 K is regarded to be the same as that of NpSSNp. When the ambient

TABLE 1: Decay Rate Constants of NpSSNp NpSSNp$^{\bullet-}$ Obtained at Various Temperatures

T^a/K	$k_d{}^b/10^5$ s^{-1}
160	1.00
180	3.04
200	3.24
250	6.41
293	18.6

[a] ±1.0 °C. [b] Errors ±5%.

temperature increased, the decreased viscosity of the solvent allows the free molecular motion of NpSSNp$^{\bullet-}$, such as elongation of the S−S bond or rotational motion of the naphthyl groups along the S−S bond axial. On going from NpSSNp to NpSSNp$^{\bullet-}$, the change ratio in the CSSC twist angel is 8% and that in the S−S distance is 36%. From the great change in the S−S bond length of NpSSNp$^{\bullet-}$ at 77 and 100 K, it is inferred that the difference in the wavelength of the absorption bands at 77 and 100 K is reflected by the conformational changes. Shida reported a reversible absorption change of dimethyl disulfide radical anion (MeSSMe$^{\bullet-}$) during photoirradiation in MTHF at 77 K.[29] The mechanism was proposed to be rotational isomerization along the S−S bond axis, which is different from that for the present NpSSNp$^{\bullet-}$.

To understand the effect of the ambient temperature change on the properties of NpSSNp$^{\bullet-}$, the temperature dependence of the decay rate constant, k_d, of NpSSNp$^{\bullet-}$ leading to the formation of NpS$^{\bullet}$ and NpS^{-} was examined in a temperature range from 160 to 293 K. The obtained k_d values within ±5% errors are listed in Table 1. Figure 4 shows the Arrhenius plots of k_d. Since the plots gave a straight line, k_d is expressed by

$$\ln k_d = \ln A - \Delta E_a (RT)^{-1} \quad (4)$$

where A and ΔE_a denote a frequency factor and an apparent activation energy for the S−S bond cleavage in NpSSNp$^{\bullet-}$, respectively. From the slope and intercept of the line, the values of ΔE_a and A for the S−S bond cleavage in NpSSNp$^{\bullet-}$ were determined to be 1.8 kcal mol^{-1} and 3.4×10^7 s^{-1}, respectively.

It is shown that RSSR$^{\bullet-}$ is a three-electron-bonded radical where a bonding σ molecular orbital is doubly occupied, and the corresponding antibonding σ, i.e., σ^*, orbital is singly occupied. The orbital occupation between the two sulfur atoms is expressed as $\sigma(2)\sigma^*(1)$.[30] The antibonding σ^* electron is responsible for the weakened S−S bond and the facile bond cleavage. Theoretical studies provide useful information on the electronic mechanism involved in the S−S bond cleavage in the gas phase. A number of theoretical approaches to the mesolytic bond dissociation in RSSR$^{\bullet-}$ have been reported.[23,30−33] The energy potential, ΔE^{RA}, of the three-electron-bonded RSSR$^{\bullet-}$ having a S−S bond dissociation energy, BDE^{RA}, can be described by using a Morse potential expressed by[23,31−34]

$$\Delta E^{RA} = \mathrm{BDE}^{RA}(1 - \exp(-\beta(r - r_e)))^2 \quad (5)$$

where β, r, and r_e denote a Morse constant, the S−S bond distance, and the equilibrium S−S bond distance (0.290 nm), respectively, for NpSSNp$^{\bullet-}$ in the gas phase. The ΔE^{RA} values were calculated at the B3LYP/6-31G(d) level as a function of r, and plotted in Figure 5. The calculated total energies of NpSSNp$^{\bullet-}$ are provided in the Supporting Information. The energy profile can be constructed according to a Morse potential function of eq 5 with the use of the best-fitted values of β = 12.8 nm^{-1} and BDE^{RA} = 6.7 kcal mol^{-1}. NpSSNp$^{\bullet-}$ is formed from the electron-attachment at the S−S bond distance of 0.213 nm the equilibrium distance of NpSSNp. As the state energy of NpSSNp$^{\bullet-}$ becomes lower along the potential curve, the S−S bond length elongates from 0.213 to 0.290 nm. The S−S bond elongation on going from the two-electron bond of RSSR to the three-electron bond of the corresponding radical anion, RSSR$^{\bullet-}$ is supported by theoretical calculations. HS−SH increases the S−S bond length from 0.207 to 0.283 nm,[32] MeS−SMe from 0.204 to 0.280 nm,[33] and PhS−SPh from 0.209 to 0.289 nm.[31] It is reported that the increase of the bond length is matched by a decrease in the BDE value.[23] The BDE values of the diphenyl disulfide radical anion (PhSSPh$^{\bullet-}$) and its derivatives are reported to be 10−16 kcal mol^{-1},[31,35] which are somewhat larger than the estimated BDE value of NpSSNp$^{\bullet-}$ in the gas phase (6.7 kcal mol^{-1}). Considering the S−S bond length of NpSSNp$^{\bullet-}$ is 0.290 nm, the estimated BDE value for NpSSNp$^{\bullet-}$ seems to obey the reported relationship between the BDE and the S−S bond distance of the radical anions. In the present study, we have determined the apparent activation energy, ΔE_a being 1.8 kcal mol^{-1} along the frequency factor ($A = 3.4 \times 10^7$ s^{-1}) in MTHF solution. Assuming that the S−S bond cleavage of NpSSNp$^{\bullet-}$ in solution proceeds along with the Morse-like potential, the actual BDE of NpSSNp$^{\bullet-}$ should be as small as the ΔE_a value. The obtained frequency factor may correspond to the vibrational frequency of the S−S bond going over the potential barrier (ΔE_a) for the bond fission leading to the formation of NpS$^{\bullet}$ and NpS^{-}.

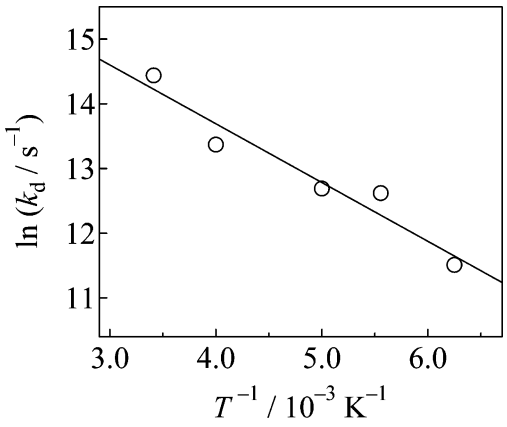

Figure 4. Arrhenius plots of the decay rate constants, k_d, of NpSSNp$^{\bullet-}$ obtained during the pulse radiolysis of NpSSNp in MTHF in the temperature range 160−293 K.

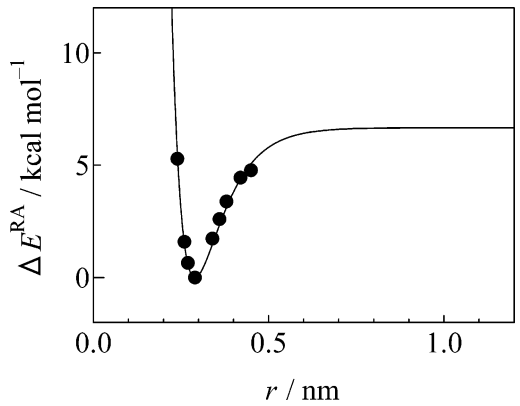

Figure 5. Energy profile for the S−S bond cleavage in NpSSNp$^{\bullet-}$ as a function of the S−S bond distance, r. The solid curve was drawn by eq 5 using BDE^{RA} = 6.7 kcal mol^{-1} and β = 12.8 nm^{-1}. The data points (●) refer to the corresponding stationary-point calculations at the B3LYP/6-31G(d) level.

The β values of other $RSSR^{\bullet-}$ species are reported to be 0.116 nm^{-1} for $MeSSMe^{\bullet-}$ [33] and 0.141[31] or 0.103 nm^{-1} [33] for $PhSSPh^{\bullet-}$, which are substantially smaller than that for $NpSSNp^{\bullet-}$ (12.8 nm^{-1}). In principle, based on the vibrational analysis of a diatomic oscillating system,[35] the β value for a radical anion of the S−S bond having the BDE^{RA} is equal to the second derivative of the potential function at the equilibrium distance, $r = r_e$,

$$\beta = (k/2\mathrm{BDE}^{\mathrm{RA}})^{1/2} \quad (6)$$

where k is the force constant for stretching motion between two S atoms. Considering that the estimated BDE of $NpSSNp^{\bullet-}$ is approximately half or one-third of the BDEs of the smaller $RSSR^{\bullet-}$ in the gas phase, a much larger force constant of $NpSSNp^{\bullet-}$ would contribute to the larger β value of $NpSSNp^{\bullet-}$ than those of the smaller $RSSR^{\bullet-}$. On the other hand, the vibrational frequency (ν_e) of the stretching between the S−S bond is given by[36]

$$\nu_e = (1/2\pi)(k/\mu)^{1/2} \quad (7)$$

where μ is the reduced mass of two S atoms. With the dihydrogen disulfide radical anion ($HSSH^{\bullet-}$) as the simplest $RSSR^{\bullet-}$, the ν_e is calculated to be ca. 220 cm^{-1} in the gas phase,[32] which corresponds to a rate constant of ca. 6×10^{12} s^{-1}. Assuming that the stretching between the S−S bond promotes the S−S bond cleavage in the radical anions and considering that the force constant of $NpSSNp^{\bullet-}$ is much larger than those of the smaller $RSSR^{\bullet-}$, the naphthyl group of $NpSSNp^{\bullet-}$ in solution may prevent a fast separation of $NpSSNp^{\bullet-}$ into $NpS^{\bullet}$ and NpS^{-} due to the viscosity of the surrounding solvent. In aqueous solution, the rate constants for the dissociation of the disulfide linkage of $RSSR^{\bullet-}$ are reported to be on the order of 10^5 s^{-1} [16a] whereas dynamics parameters such as Arrhenius parameters are lacking due to the limited temperature range of these experiments. To understand the properties of the S−S bond mesolysis of $RSSR^{\bullet-}$, further studies of RSSR having bulky substituents are in progress.

4. Conclusions

$NpSSNp^{\bullet-}$ generated during the γ-radiolysis in MTHF at 77 K showed an absorption band at 430 nm, which shifted to 560 nm with an increase of the ambient temperature to 273 K. DFT calculations showed that the shift was due to molecular conformational changes of $NpSSNp^{\bullet-}$ whose S−S bond elongates to be a length of 0.290 nm in fluid phase compared with that of 0.213 nm in a rigid matrix at 77 K.[36] It was confirmed that $NpSSNp^{\bullet-}$ undergoes S−S bond cleavage to form $NpS^{\bullet}$ and NpS^{-} with a first-order rate constant in the magnitude of 10^6 s^{-1} in solution at room temperature. The activation energy, ΔE_a for the S−S bond cleavage in $NpSSNp^{\bullet-}$ was determined to be 1.8 kcal mol^{-1} along with a frequency factor of 3.4×10^7 s^{-1}. A calculated energy potential for the S−S bond dissociation of $NpSSNp^{\bullet-}$ in the gas phase is drawn in Figure 5. The BDE of the S−S bond for $NpSSNp^{\bullet-}$ in the gas phase was extrapolated from the calculated state energies to be 6.7 kcal mol^{-1}, and the actual BDE value in solution is suggested to be as small as ΔE_a (1.8 kcal mol^{-1}). The slow bond cleavage of $NpSSNp^{\bullet-}$ in solution may be due to the steric hindrance of the naphthyl group upon the S−S bond stretching motion.

Acknowledgment. We thank all members in the Radiation Laboratory, The Institute of Scientific and Industrial Research, Osaka University, for running the pulse radiolysis. This work has been partly supported by a Grant-in-Aid for Scientific Research (17105005), Priority Area (417), 21st Century COE Research (SANKEN), and others from the Ministry of Education, Culture, Sports, Science and Technology (MEXT) of the Japanese Government.

Supporting Information Available: Optimized molecular structure of NpSSNp and table of heats of formation, state energy, and dihedral angles. This material is available free of charge via the Internet at http://pubs.acs.org.

References and Notes

(1) Conn, E. E.; Stumpf, P. K.; Bruening, G.; Doi, R. H. *Outlines of Biochemistry*; Wiley: New York, 1987.
(2) Faraggi, M.; Klapper, M. H.; Dorfman, L. M. *J. Phys. Chem.* **1978**, *82*, 508 and references cited therein.
(3) Froni, L. G.; Willson, R. L. *Biochem. J.* **1986**, *240*, 897.
(4) Wilkening, V. G.; Lal, M.; Arends, M.; Armstrong, D. A. *Can. J. Chem.* **1967**, *45*, 1209.
(5) Al-Thannon, A.; Peterson, R. M.; Trumbore, C. N. *J. Phys. Chem.* **1968**, *92*, 2395.
(6) Packer, J. E.; Winchester, R. V. *Can. J. Chem.* **1970**, *48*, 417.
(7) Purde, J. W. *Can. J. Chem.* **1971**, *49*, 725.
(8) Armstrong, W. A.; Humphreys, W. G. *Can. J. Chem.* **1967**, *45*, 2589.
(9) Wolf, W.; Kertesz, J. C. *J. Magn. Resonan.* **1969**, *1*, 618.
(10) Neta, P.; Fessenden, R. W. *J. Phys. Chem.* **1971**, *75*, 2277.
(11) Nucifora, G.; Smaller, B.; Remko, R.; Avery, E. C. *Radiat. Res.* **1972**, *49*, 96.
(12) Braams, R. *Radat. Res.* **1966**, *27*, 319.
(13) (a) Adams, G. E.; McNaughton, G. S.; Michael, B. D. *Trans. Faraday Soc.* **1968**, *64*, 902. (b) Adams, G. E.; Armstrong, R. C.; Charlesby, A.; Michael, B. D.; Willson, R. L. *Trans. Faraday Soc.* **1969**, *65*, 732.
(14) Barton, J. P.; Packer, J. E. *Int. J. Radiat. Phys. Chem.* **1970**, *2*, 159.
(15) Purde, J. W.; Gillis, H. A.; Klassen, N. V. *Chem. Commun.* **1971**, 1163.
(16) (a) Hoffman, M. Z.; Hayon, E. *J. Am. Chem. Soc.* **1972**, *94*, 7950. (b) Hoffman, M, Z.; Hayon, E. *J. Phys. Chem.* **1973**, *77*, 990.
(17) Purde, J. W.; Gillis, H. A.; Klassen, N. V. *Can. J. Chem.* **1973**, *51*, 3132
(18) (a) Karmann, W.; Henglein, A. *Ber. Bunsen-Ges. Phys. Chem.* **1967**, *71*, 421. (b) Karmann, W.; Granzow, A.; Meissner, G.; Henglein, A. *Int. J. Radiat. Phys. Chem.* **1969**, *1*, 395.
(19) Caspari, G.; Granzow, A. *J. Phys. Chem.* **1970**, *74*, 836.
(20) Braams, R. *Radiat. Res.* **1966**, *27*, 319.
(21) Favaudon, V.; Tourbez, H.; Houée-Levin, C.; Lhoste, J.-M. *Biochemistry* **1990**, *29*, 10978.
(22) Mezyk, S. P. *J. Phys. Chem.* **1995**, *99*, 13970.
(23) Maran, F.; Wayner, D. D. M.; Workentin, M. S. *Adv. Phys. Org. Chem.* **2001**, *36*, 85.
(24) Lu, C.; Bucher, G.; Sander, W. *Chem. PhysChem.* **2004**, *5*, 399.
(25) Yoshikawa, Y.; Watanabe, A.; Ito, O. *J. Photochem. Photobiol. A:Chem.* **1995**, *89*, 209.
(26) Tachikawa, T.; Tojo, S.; Fujitsuka, M.; Majima, T. *J. Phys. Chem. B* **2005**, *109*, 17460.
(27) Frisch, M. J.; Trucks, G. W.; Schlegel, H. B.; Scuseria, G. E.; Robb, M. A.; Cheeseman, J. R.; Montgomery, J. A., Jr.; Vreven, T.; Kudin, K. N.; Burant, J. C.; Millan, J. M.; Iyanger, S. S.; Tomasi, J.; Baron, J.; Mennucci, B.; Cossi, M.; Scalmani, G.; Rega, N.; Petersson, G. A.; Nakatsuji, H.; Hada, M.; Ehara, M.; Toyota, K.; Fukuda, R.; Hasegawa, J.; Ishida, M.; Nakajima, T.; Honda, Y.; Kitao, O.; Nakai, H.; Klene, M.; Li, X.; Knox, J. E.; Hratchian, H. P.; Cross, J. B.; Adamo, C.; Jaramillo, J.; Gomperts, R.; Stratmann, R. E.; Yazyev, O.; Austin, A. J.; Cammi, R.; Pomelli, C.; Ochterski, J. W.; Ayala, P. Y.; Morokuma. K.; Voth, G. A.; Salvador, P.; Dannenberg, J. J.; Zakrzewski, V. G.; Dapprich, S.; Daniel, A. D.; Strain, M. C.; Farkas, O.; Malick, D. K.; Rabuck, A. D.; Raghavachari, K.; Foresman, J. B.; Ortiz, J. V.; Cui, Q.; Baboul, A. G.; Clifford, S.; Cioslowski, J.; Stefanov, B. B.; Liu, G.; Liashenko, A.; Piskorz, P.; Komaromi, I.; Martin, R. L.; Fox, D. J.; Keith, T.; Al-Laham, M. A.; Peng, C. Y.; Nanayakkara, A.; Challacombe, M.; Gill, M. M. W.; Johnson, B.; Chen, W.; Wong, M. W.; Gonzalez, C.; Pople, J. A. *GAUSSIAN 03*, revision B.05; Gaussian, Inc.: Pittsburgh, PA, 2003.
(28) Yamaji, M.; Ueda, S.; Shizuka, H.; Tobita, S. *Phys. Chem. Chem. Phys.* **2001**, *3*, 3102
(29) Shida, T. *J. Phys. Chem.* **1968**, *72*, 2597.
(30) Göbl, M.; Bonifacic, M.; Asmus, K.-D. *J. Am. Chem. Soc.* **1984**, *106*, 5984.

(31) Antonello, S.; Daasbjerg, K.; Jensen, H.; Taddei, F.; Maran, F. *J. Am. Chem. Soc.* **2003**, *125*, 14905.

(32) German, E. D.; Kuznetsov, A. M. *J. Phys. Chem. A* **1998**, *102*, 3668.

(33) Benassi, R.; Taddel, F. *J. Phys. Chem. A* **1998**, *102*, 6173.

(34) Antonello, S.; Benassi, R.; Gavioli, G.; Taddei, F.; Maran, F. *J. Am. Chem. Soc.* **2002**, *124*, 7529.

(35) Daubel, R.; Leroy, G.; Peeters, D.; Sana, M. *Quantum Chemistry*; John Wiely and Sons: Chichester, U.K., 1983.

(36) One reviewer commented that B3LYP is incapable of DFT calculations for three-electron radical ions, referring to refs 37 and 38. Calculations at the BH&HLYP/6-31.G* level were performed for $NpSSNp^{\bullet-}$, providing that the equilibrium distance, r_e, was 0.285 nm, which was almost the same as that (0.290 nm) obtained at the B3LYP/6-31G(d) level.

(37) Bally, T.; Sastry, G. N. *J. Phys. Chem.* **1997**, *101*, 7923.

(38) Braida, B.; Hilbery, P. C.; Savin, A. *J. Phys. Chem.* **1998**, *102*, 7872.